Immunity, Volume *52*

Supplemental Information

Precursors for Nonlymphoid-Tissue Treg Cells Reside in Secondary Lymphoid Organs and Are Programmed by the Transcription Factor BATF

Michael Delacher, Charles D. Imbusch, Agnes Hotz-Wagenblatt, Jan-Philipp Mallm, Katharina Bauer, Malte Simon, Dania Riegel, André F. Rendeiro, Sebastian Bittner, Lieke Sanderink, Asmita Pant, Lisa Schmidleithner, Kathrin L. Braband, Bernd Echtenachter, Alexander Fischer, Valentina Giunchiglia, Petra Hoffmann, Matthias Edinger, Christoph Bock, Michael Rehli, Benedikt Brors, Christian Schmidl, and Markus Feuerer

Figure S1

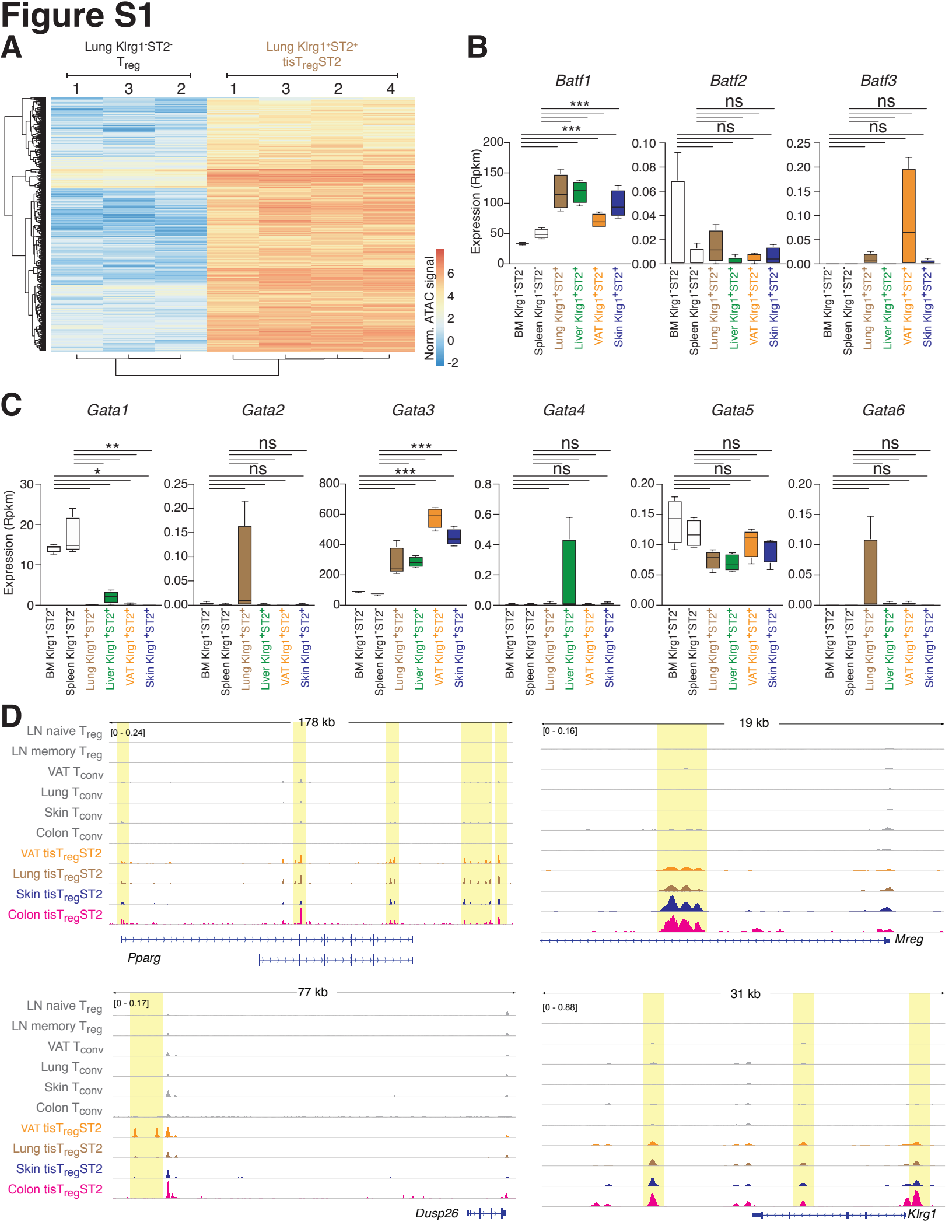
A
Lung Klrg1-ST2- Treg
Lung Klrg1+ST2+ tisTregST2
1 3 2 1 3 2 4
Norm. ATAC signal
6 4 2 0 -2
B
Batf1
Batf2
Batf3
***
***
ns
ns
ns
ns
Expression (Rpkm)
200 150 100 50 0
0.10 0.08 0.06 0.04 0.02 0.00
0.25 0.20 0.15 0.10 0.05 0.00
BM Klrg1-ST2-
Spleen Klrg1-ST2-
Lung Klrg1+ST2+
Liver Klrg1+ST2+
VAT Klrg1+ST2+
Skin Klrg1+ST2+
C
Gata1
Gata2
Gata3
Gata4
Gata5
Gata6
**
*
ns
ns
***
***
ns
ns
ns
ns
ns
ns
Expression (Rpkm)
30 20 10 0
0.25 0.20 0.15 0.10 0.05 0.00
800 600 400 200 0
0.8 0.6 0.4 0.2 0.0
0.20 0.15 0.10 0.05 0.00
0.20 0.15 0.10 0.05 0.00
BM Klrg1-ST2-
Spleen Klrg1-ST2-
Lung Klrg1+ST2+
Liver Klrg1+ST2+
VAT Klrg1+ST2+
Skin Klrg1+ST2+
D
178 kb
[0 - 0.24]
LN naive Treg
LN memory Treg
VAT Tconv
Lung Tconv
Skin Tconv
Colon Tconv
VAT tisTregST2
Lung tisTregST2
Skin tisTregST2
Colon tisTregST2
Pparg
19 kb
[0 - 0.16]
Mreg
77 kb
[0 - 0.17]
Dusp26
31 kb
[0 - 0.88]
Klrg1

Figure S1. ATAC-seq and RNA-seq of tissue-derived T cells, related to Figure 1. (**A**) Lung-derived Klrg1^{-}ST2^{-} Treg cells as well as lung Klrg1^{+}ST2^{+} tisTregST2 cells were FACS-sorted and subjected to ATAC-sequencing. Samples were normalized and reads for each sample in the "core tisTregST2" peak set derived from Figure 1D were counted. Heatmap with unsupervised clustering shows normalized ATAC signal with color code high (red) vs low (blue) (n=3-4). (**B**) *Batf1-3* gene expression in BM and spleen-derived Klrg1^{-}ST2^{-} Treg (black) as well as lung, liver, visceral adipose tissue (VAT), and skin-derived Klrg1^{+}ST2^{+} tisTregST2 (brown, green, orange and dark blue). Statistics based on Deseq2. Asterisks indicate statistical significance, with Benjamini-Hochberg correction, ***p<0.001, **p<0.01, *p<0.05 and ns p>0.05) (n=3-4). **(C)** *Gata1-6* gene expression in BM and spleen-derived Klrg1^{-}ST2^{-} Treg (black) as well as liver, lung, VAT, and skin-derived Klrg1^{+}ST2^{+} tisTregST2 (brown, green, orange, and dark blue). Colors indicate cell type (n=3-4). (**D**) ATAC-seq data for the *Klrg1*, *Pparg*, *Mreg* and *Dusp26* gene loci from lymph node (LN)-derived CD25^{+}*Foxp3*(GFP)$^{+}$CD44^{-} naive Treg, LN-derived CD25^{+}*Foxp3*(GFP)$^{+}$CD44^{+} memory Treg as well as VAT, lung, skin and colon-derived CD25^{-}*Foxp3*(GFP)$^{-}$CD44^{+} memory Tconv or CD25^{+}*Foxp3*(GFP)$^{+}$CD44^{+}Klrg1^{+}ST2^{+} tisTregST2 (n=4). Y-axis ATAC signal intensity, x-axis gene structure, with exons indicated as heightened bars and introns as line, arrows indicate gene direction. All datasets group-normalized to maximum peak height indicated in brackets. Overall display length indicated on top in kilobases (kb). Yellow box indicates area of interest. Data representative of two or more independent experiments or cell sorts.

Figure S2

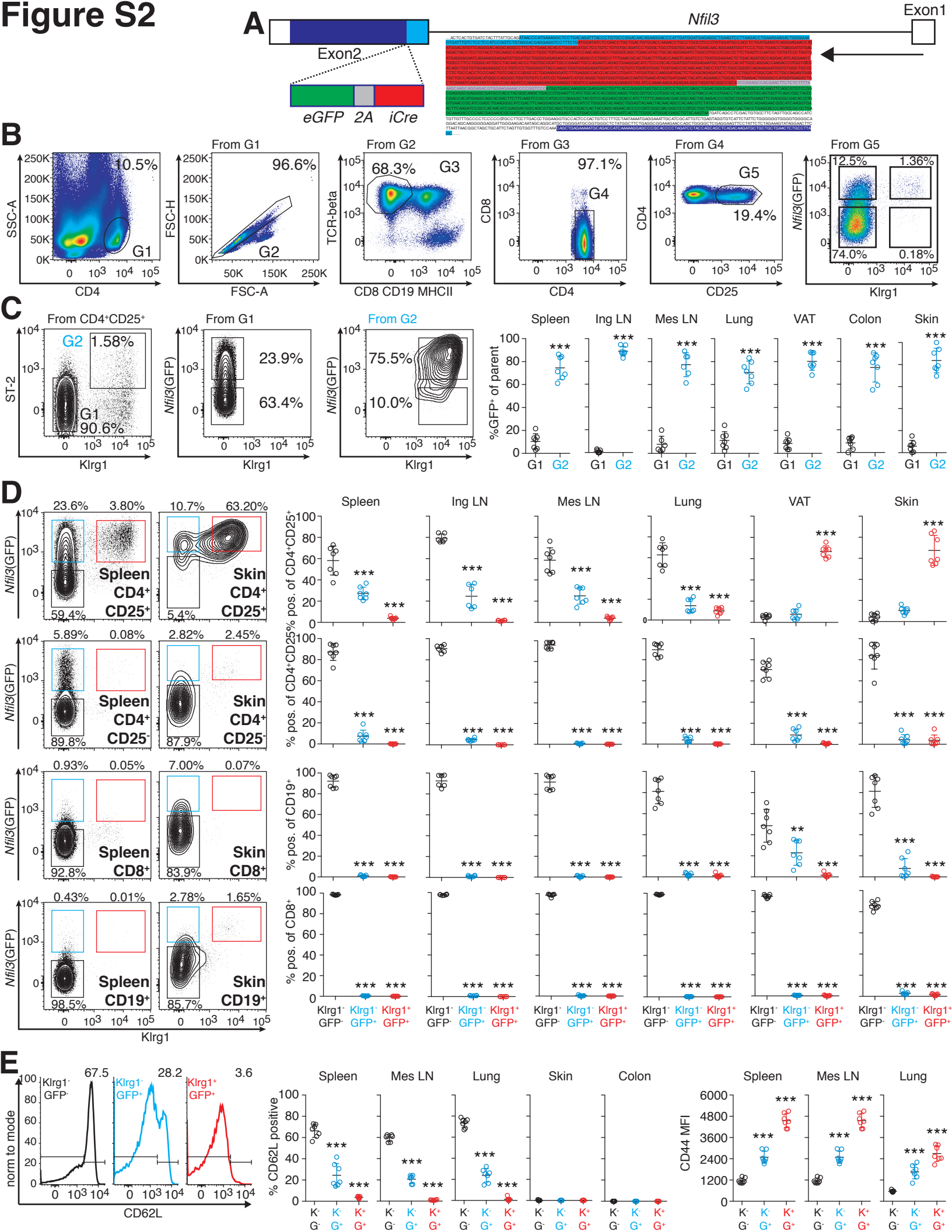
A
Nfil3
Exon1
Exon2
eGFP 2A iCre
B
From G1
From G2
From G3
From G4
From G5
SSC-A
FSC-H
FSC-A
TCR-beta
CD8 CD19 MHCII
CD8
CD4
CD25
Klrg1(GFP)
Klrg1
10.5%
96.6%
68.3%
G3
97.1%
G4
G5
19.4%
12.5%
1.36%
74.0%
0.18%
C
From CD4+CD25+
From G1
From G2
ST-2
Nfil3(GFP)
Klrg1
G2
1.58%
G1
90.6%
23.9%
63.4%
75.5%
10.0%
Spleen
Ing LN
Mes LN
Lung
VAT
Colon
Skin
%GFP+ of parent
G1
G2
D
Nfil3(GFP)
Klrg1
23.6%
3.80%
59.4%
Spleen CD4+ CD25+
10.7%
63.20%
5.4%
Skin CD4+ CD25+
5.89%
0.08%
89.8%
Spleen CD4+ CD25-
2.82%
2.45%
87.9%
Skin CD4+ CD25-
0.93%
0.05%
92.8%
Spleen CD8+
7.00%
0.07%
83.9%
Skin CD8+
0.43%
0.01%
98.5%
Spleen CD19+
2.78%
1.65%
85.7%
Skin CD19+
% pos. of CD4+CD25+ pos. of CD4+CD25+
% pos. of CD4+CD25+
% pos. of CD19+
% pos. of CD8+
Klrg1- GFP-
Klrg1- GFP+
Klrg1+ GFP+
E
norm to mode
CD62L
67.5
28.2
3.6
% CD62L positive
CD44 MFI
K- G-
K- G+
K+ G+

Figure S2. Nfil3-GFP reporter mouse, related to Figure 2. (A) Overview of insert into the BAC construct used for generating the *Nfil3*^{GFP} reporter mouse. A fusion construct composed of the DNA for *iCre* (red), *2A* (grey), and *eGFP* (green) was generated, and inserted at the start codon of the *Nfil3* gene in the BAC RP23-227M5 using *Escherichia coli* DH10B. Top, gene structure and insertion site. Bottom, DNA code inserted into BAC. (**B**) Gating strategy used to identify Treg cells in *Nfil3*^{GFP} reporter or control mice (data derived from lymph node). G1: CD4$^+$ T cells; G2: single cells; G3: CD8$^-$CD19$^-$MHCII$^-$Dead$^-$TCRbeta$^+$ T cells; G4: CD4$^+$CD8$^-$ T cells; G5: CD4$^+$CD25$^+$ Treg cells. (**C**) Expression of *Nfil3*(GFP) in Klrg1$^+$ST2$^+$ tisTregST2 (G2) vs Klrg1$^-$ST2$^-$ Treg cells (G1) from various tissues (paired t test, ing LN = inguinal LN; mes LN = mesenteric LN, n=7). (**D**) Presence of Klrg1$^+$*Nfil3*(GFP)$^+$ Treg cells (red gate), Klrg1$^-$*Nfil3*(GFP)$^+$ Treg cells (light blue gate), and Klrg1$^-$*Nfil3*(GFP)$^-$ Treg cells (black gate) in different cell populations. First row: CD4$^+$CD25$^+$ Treg cells; Second row: CD4$^+$CD25$^-$ Tconv cells; Third row: CD8$^+$ cytotoxic T cells; Fourth row: CD19$^+$ B cells. Contour plots to the left show presence of populations in spleen or skin. Additional data points, tissues and statistical evaluation shown in the graphs to the right (one-way ANOVA with Tukey correction, n=7). (**E**) Memory phenotype of Klrg1$^-$*Nfil3*(GFP)$^-$ Treg cells (black), Klrg1$^-$*Nfil3*(GFP)$^+$ Treg cells (blue) and Klrg1$^+$*Nfil3*(GFP)$^+$ Treg cells (red). Left, histograms illustrating expression of CD62L in spleen-derived Treg cell populations. Middle, additional data points, tissues and statistical evaluation (one-way ANOVA with Tukey correction, n=7). Right, CD44 MFI for Treg populations in spleen, mes LN and lung (one-way ANOVA with Tukey correction, n=7). Data representative of two or more independent experiments or cell sorts.

Figure S3

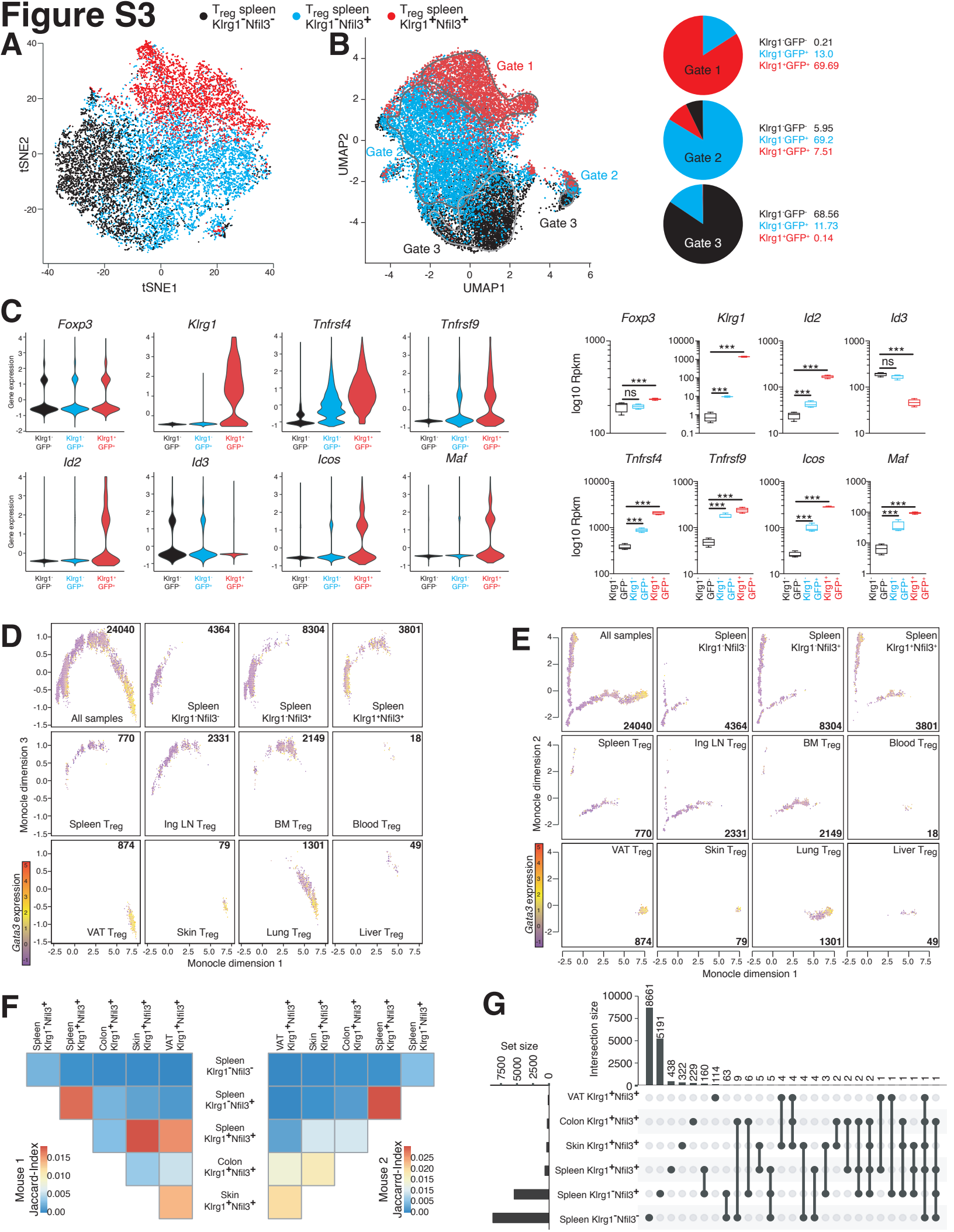
A
B
C
D
E
F
G
Treg spleen Klrg1-Nfil3-
Treg spleen Klrg1-Nfil3+
Treg spleen Klrg1+Nfil3+
tSNE1
tSNE2
UMAP1
UMAP2
Gate 1
Gate 2
Gate 3
Klrg1-GFP- 0.21
Klrg1-GFP+ 13.0
Klrg1+GFP+ 69.69
Klrg1-GFP- 5.95
Klrg1-GFP+ 69.2
Klrg1+GFP+ 7.51
Klrg1-GFP- 68.56
Klrg1-GFP+ 11.73
Klrg1+GFP+ 0.14
Foxp3
Klrg1
Tnfrsf4
Tnfrsf9
Id2
Id3
Icos
Maf
Gene expression
log10 Rpkm
ns
***
All samples
Spleen Klrg1-Nfil3-
Spleen Klrg1-Nfil3+
Spleen Klrg1+Nfil3+
Spleen Treg
Ing LN Treg
BM Treg
Blood Treg
VAT Treg
Skin Treg
Lung Treg
Liver Treg
Monocle dimension 1
Monocle dimension 2
Monocle dimension 3
Gata3 expression
Mouse 1 Jaccard-Index
Mouse 2 Jaccarrd-Index
Set size
Intersection size

Figure S3. ScRNA-seq and scTCR-seq of tissue T cells, related to Figure 2+3. (**A**) t-Distributed Stochastic Neighbor Embedding (t-SNE) of single-cell RNA-sequencing data of spleen-derived Treg cell ($CD4^+TCR\beta^+CD25^+$) subpopulations: $Klrg1^-$*Nfil3*$(GFP)^-$ in black, $Klrg1^-$*Nfil3*$(GFP)^+$ in blue, and $Klrg1^+$*Nfil3*$(GFP)^+$ in red (n=5). (**B**) Uniform manifold approximation and projection (UMAP) of single-cell RNA-sequencing data of spleen-derived Treg cell ($CD4^+TCR\beta^+CD25^+$) subpopulations as in (A). Contour gates were drawn to include 70% of the parent population (Gate 1-3). Contribution of cell types to Gate1-3 shown in the pie charts to the right (n=5). (**C**) Violin plots illustrating the expression of *Foxp3*, *Klrg1*, *Id2*, *Id3*, *Tnfrsf4*, *Tnfrsf9*, *Icos*, and *Maf* in $Klrg1^-$*Nfil3*$(GFP)^-$ Treg, $Klrg1^-$*Nfil3*$(GFP)^+$ Treg, and $Klrg1^+$*Nfil3*$(GFP)^+$ Treg as in (F-G). Violin plots were scaled by width resulting in the same maximum width for all violins. Right, gene expression data of $Klrg1^-$*Nfil3*$(GFP)^-$ Treg cells (black), $Klrg1^-$*Nfil3*$(GFP)^+$ Treg cells (blue) and $Klrg1^+$*Nfil3*$(GFP)^+$ Treg cells (red) for *Foxp3*, *Klrg1*, *Id2*, *Id3*, *Tnfrsf4*, *Tnfrsf9*, *Icos*, and *Maf*. Statistics based on Deseq2 (n=4). **(D)** Monocle plots derived from scRNA-seq data of spleen $Klrg1^-$*Nfil3*$(GFP)^-$ Treg, spleen $Klrg1^-$*Nfil3*$(GFP)^+$ Treg, spleen $Klrg1^+$*Nfil3*$(GFP)^+$ Treg as well as spleen, inguinal LN (ing LN), bone marrow, blood, VAT, skin, lung, and liver memory Treg ($CD4^+TCR\beta^+CD44^+CD25^+$*Foxp3*$(GFP)^+$). Color code indicates expression of *Gata3*. X-axis and y-axis indicate monocle dimension 1 and 3. Each dot represents a hexagonal bin, and each dot is colored by the mean expression value of *Gata3* of the cells that are within the hexagonal bin. (**E**) Pseudotime plot as in (A) with monocle dimension 1 and dimension 2. (**F**) Data derived from scTCR-seq of spleen $Klrg1^-$*Nfil3*$(GFP)^-$ Treg, spleen $Klrg1^-$*Nfil3*$(GFP)^+$ Treg, spleen $Klrg1^+$*Nfil3*$(GFP)^+$ Treg as well as colon, skin, and VAT-derived $Klrg1^+$*Nfil3*$(GFP)^+$ tisTregST2 from two individual mice. Graphical representation of similarity coefficients between these samples based on Jaccard Index for both experiments. Color indicates similarity with low (blue) to high (red) (n=2). (**G**) Data derived from scTCR-seq of VAT, colon and skin-derived $Klrg1^+$*Nfil3*$(GFP)^+$ tisTregST2 as well as spleen $Klrg1^+$*Nfil3*$(GFP)^+$ Treg, spleen $Klrg1^-$*Nfil3*$(GFP)^+$ Treg, and spleen $Klrg1^-$*Nfil3*$(GFP)^-$ Treg from an individual mouse. Set size enumerates total number of successfully identified TCR α+β chains (left). To the right, individual clones and shared clones between all groups are displayed. On top, the total number of shared clones is displayed and numbered (n=2). Data representative of two or more independent experiments or cell sorts.

Figure S4

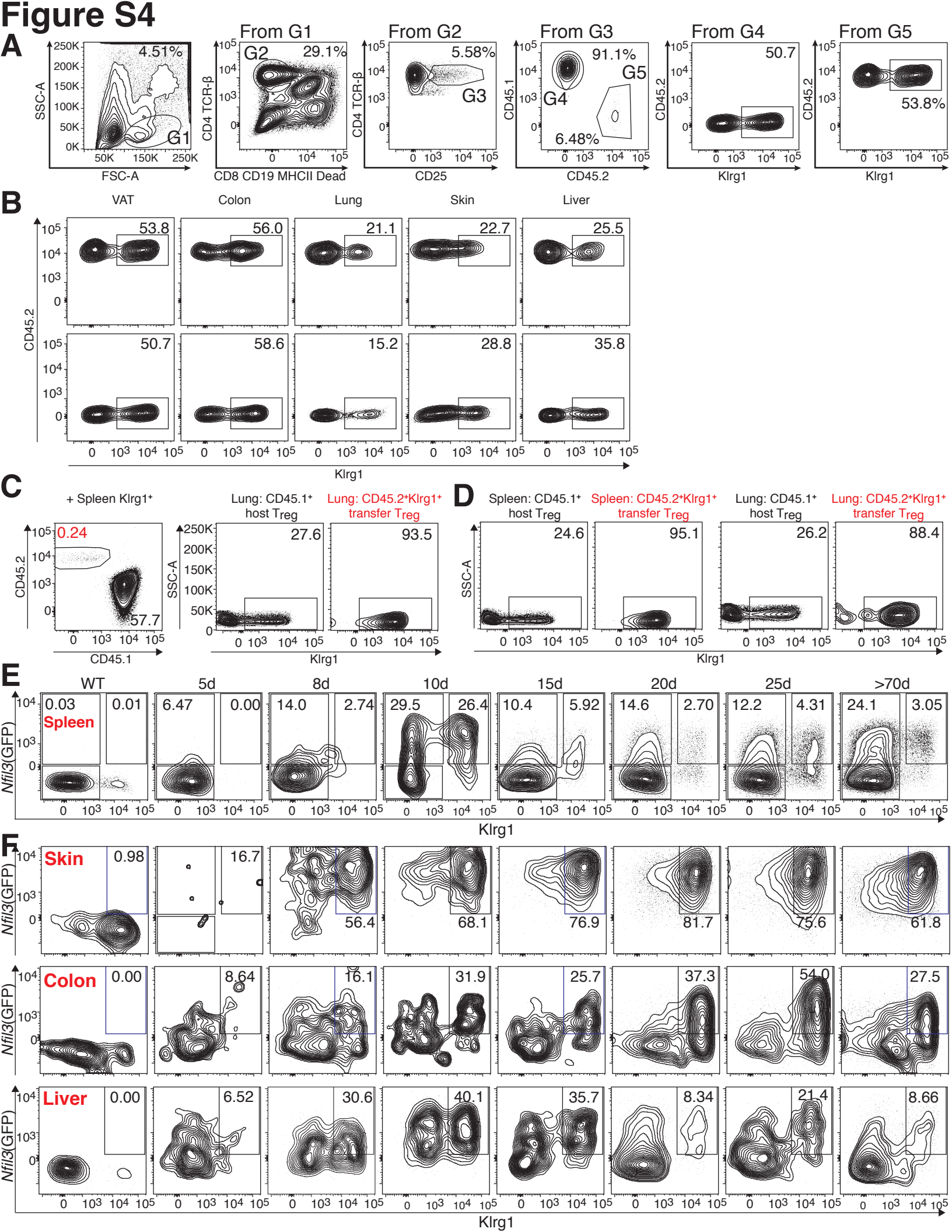
A
From G1
From G2
From G3
From G4
From G5
SSC-A
FSC-A
4.51%
G1
CD4 TCR-β
CD8 CD19 MHCII Dead
29.1%
G2
CD25
5.58%
G3
CD45.1
CD45.2
91.1%
G5
G4
6.48%
50.7
Klrg1
53.8%
B
VAT
Colon
Lung
Skin
Liver
53.8
56.0
21.1
22.7
25.5
50.7
58.6
15.2
28.8
35.8
C
+ Spleen Klrg1⁺
0.24
57.7
Lung: CD45.1⁺ host Treg
Lung: CD45.2⁺Klrg1⁺ transfer Treg
27.6
93.5
D
Spleen: CD45.1⁺ host Treg
Spleen: CD45.2⁺Klrg1⁺ transfer Treg
24.6
95.1
26.2
88.4
E
WT
5d
8d
10d
15d
20d
25d
>70d
Nfil3(GFP)
Spleen
0.03
0.01
6.47
0.00
14.0
2.74
29.5
26.4
10.4
5.92
14.6
2.70
12.2
4.31
24.1
3.05
F
Skin
0.98
16.7
56.4
68.1
76.9
81.7
75.6
61.8
Colon
0.00
8.64
16.1
31.9
25.7
37.3
54.0
27.5
Liver
0.00
6.52
30.6
40.1
35.7
8.34
21.4
8.66

Figure S4. Adoptive transfer and development, related to Figure 4. (A) Gating strategy used to identify transferred and host Treg cells in DT-treated host animals. G1: Lymphocytes; G2: $CD8^{-}$ $CD19^{-}MHCII^{-}Dead^{-}TCRbeta^{+}CD4^{+}$ T cells; G3: $TCRbeta^{+}CD4^{+}CD25^{+}$ Treg cells; G4: $CD45.1^{+}CD45.2^{-}$ host Treg cells; G5: $CD45.1^{-}CD45.2^{+}$ transferred Treg cells. Two plots to the right illustrate expression of Klrg1 in $CD45.1^{+}CD45.2^{-}$ host Treg cells and $CD45.1^{-}CD45.2^{+}$ transferred Treg cells. (**B**) Identification of transferred Treg cells in tissues of recipient animals 10 days after transfer of $CD45.2^{+}$ $Klrg1^{-}$*Nfil3*$(GFP)^{+}$ Treg cells. Contour plots illustrate expression of Klrg1 in transferred Treg (top) or host Treg (bottom). (**C**) Identification of transferred Treg cells in lung tissue of recipient animals 10 days after transfer of spleen-derived $CD45.2^{+}Klrg1^{-}$*Nfil3*$(GFP)^{+}$ Treg cells. Contour plots illustrate expression of Klrg1 in transferred and host Treg. (**D**) Identification of transferred Treg cells in spleen, mesenteric LN (Mes) and lung tissue of recipient animals 10 days after transfer of lung-derived $CD45.2^{+}Klrg1^{-}$*Nfil3*$(GFP)^{+}$ Treg cells. Contour plots illustrate expression of Klrg1 in transferred and host Treg. (**E**) Representative examples of spleen $Klrg1^{-}$ *Nfil3*$(GFP)^{+}$ and $Klrg1^{+}$*Nfil3*$(GFP)^{+}$ Treg cells 5d, 8d, 10d, 15d, 20d, 25d, and 70+d after birth. Pre-gate on $CD8^{-}CD19^{-}MHCII^{-}Dead^{-}TCRbeta^{+}CD4^{+}CD25^{+}$ Treg cells. (**F**) Representative examples of skin, colon and liver $Klrg1^{+}$*Nfil3*$(GFP)^{+}$ Treg cells 5d, 10d, 12d, 15d, 20d, 25d, and 70+d after birth. Pre-gate on $CD8^{-}CD19^{-}MHCII^{-}Dead^{-}TCRbeta^{+}CD4^{+}CD25^{+}$ Treg cells. For skin, lung and colon contour plots, flow cytometry data of several replicates were concatenated to increase visibility. Data representative of two or more independent experiments, n=3-19 per group for each experiment.

Figure S5

—Spleen T_{reg} Klrg1$^-$Nfil3$^-$ —Spleen T_{reg} Klrg1$^-$Nfil3$^+$ —Spleen T_{reg} Klrg1$^+$Nfil3$^+$ — Lung tisT_{reg}ST2 VAT tisT_{reg}ST2 Skin tisT_{reg}ST2

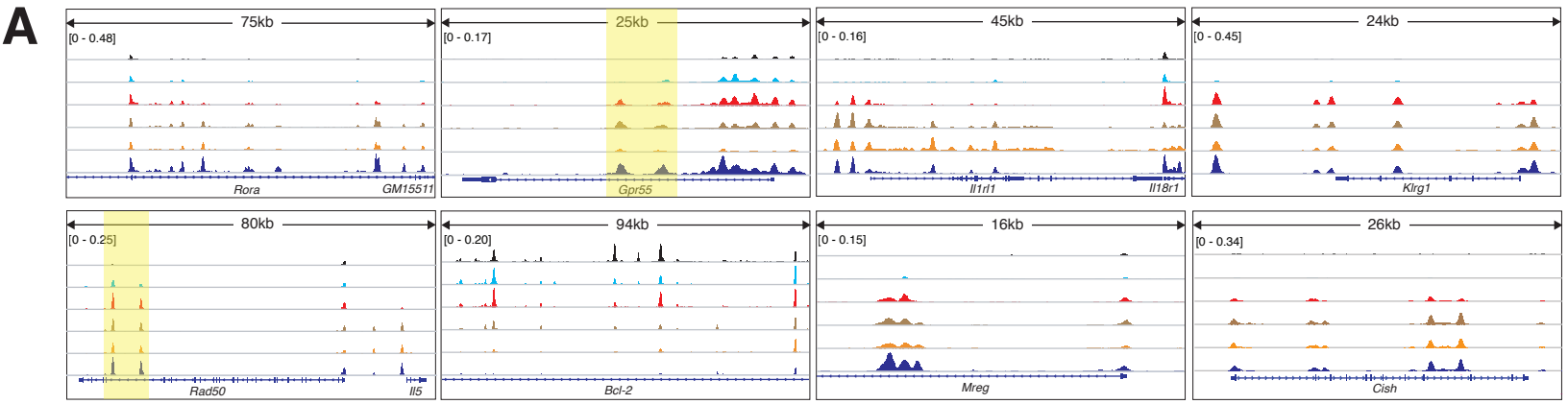

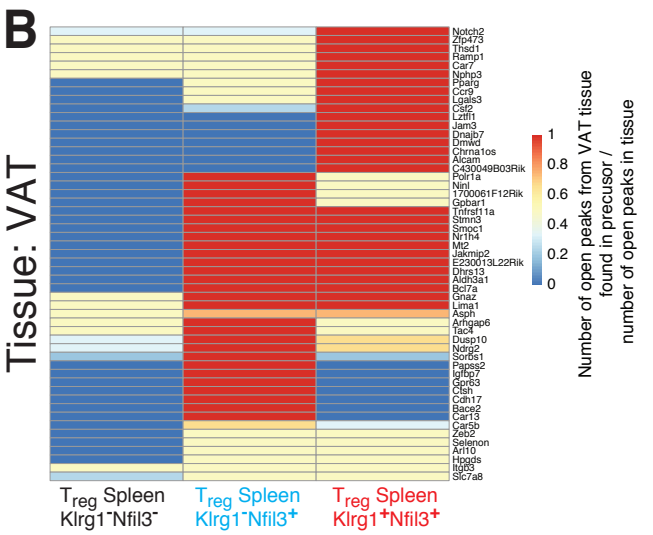

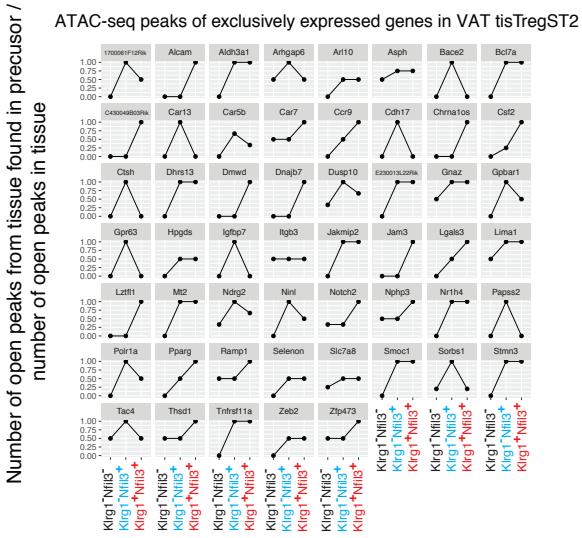

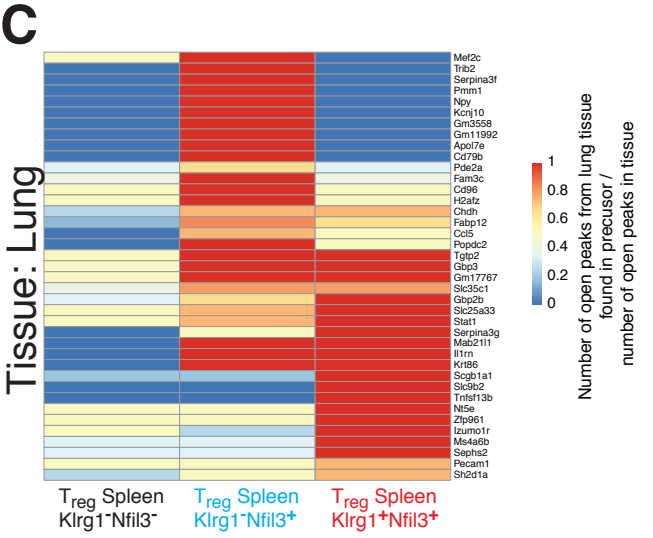

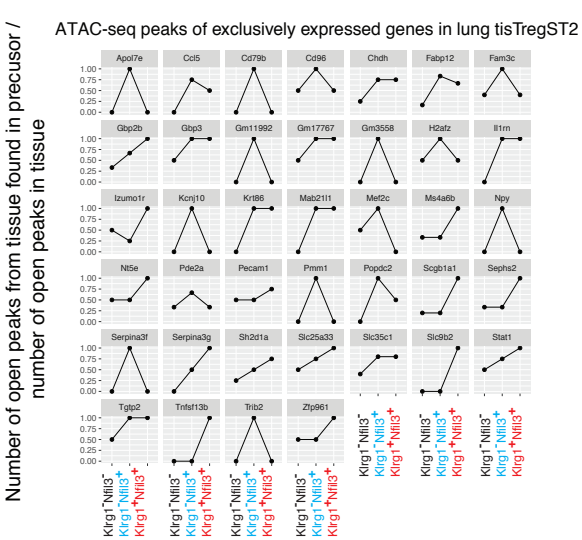

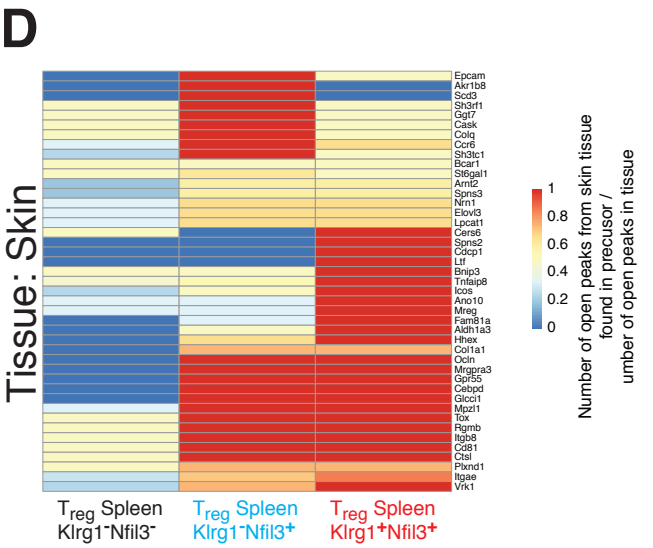

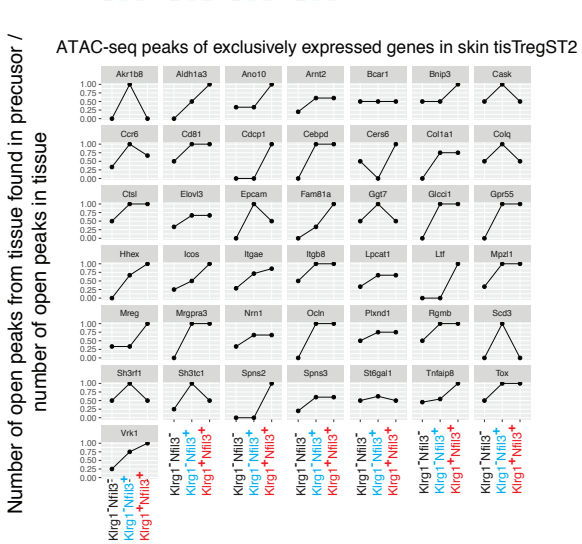

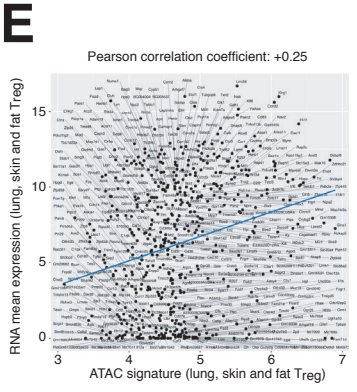

Figure S5. ATAC-seq of tissue T cells, related to Figure 5. (**A**) ATAC-seq data for parts of the *Rora*, *Gpr55*, *Rad50*, *Bcl2*, *Il1rl1, Klrg1, Mreg* and *Cish* gene loci of spleen-derived Klrg1$^-$ *Nfil3*(GFP)$^-$ Treg cells (black), spleen Klrg1$^-$*Nfil3*(GFP)$^+$ Treg cells (light blue), spleen Klrg1$^+$*Nfil3*(GFP)$^+$ Treg cells (red) as well as lung, VAT, and skin-derived CD25$^+$*Foxp3*(GFP)$^+$CD44$^+$Klrg1$^+$ST2$^+$ tisTregST2 (light brown, orange, dark blue). Y-axis ATAC signal intensity, x-axis gene structure, with exons indicated as heightened bars and introns as line, arrows indicate gene direction. All datasets group-normalized to maximum peak height indicated in brackets. Overall display length indicated on top in kilobases (kb) (n=4). (**B**) Left, heatmap illustrating number of open peaks from VAT tisTregST2 cells found in precursor/number of open peaks in VAT tissue for three groups spleen-derived Klrg1$^-$*Nfil3*(GFP)$^-$ Treg cells (black), spleen Klrg1$^-$*Nfil3*(GFP)$^+$ Treg cells (light blue), spleen Klrg1$^+$*Nfil3*(GFP)$^+$ Treg cells (red). X-axis sample type, y-axis gene name. To the right, ATAC-seq peaks of exclusively expressed genes from VAT tisTregST2 for three groups spleen-derived Klrg1$^-$*Nfil3*(GFP)$^-$ Treg cells (black), spleen Klrg1$^-$ *Nfil3*(GFP)$^+$ Treg cells (light blue) and spleen Klrg1$^+$*Nfil3*(GFP)$^+$ Treg cells (red). X-axis sample type, y-axis number of open peaks from tissue found in precursor/number of open peaks in tissue (n=4). (**C**) Heatmap illustrating number of open peaks from lung tisTregST2 found in precursor/number of open peaks in lung tissue for three groups as in (B) (n=4). (**D**) Heatmap illustrating number of open peaks from skin tisTregST2 found in precursor/number of open peaks in skin tissue for three groups as in (B) (n=4). (**E**) Correlation between common ATAC signature (Lung, skin and VAT Treg) and RNA expression (lung, skin and VAT Treg); 10kb distance to gene (n=4). Data representative of two or more independent experiments or cell sorts.

Figure S6

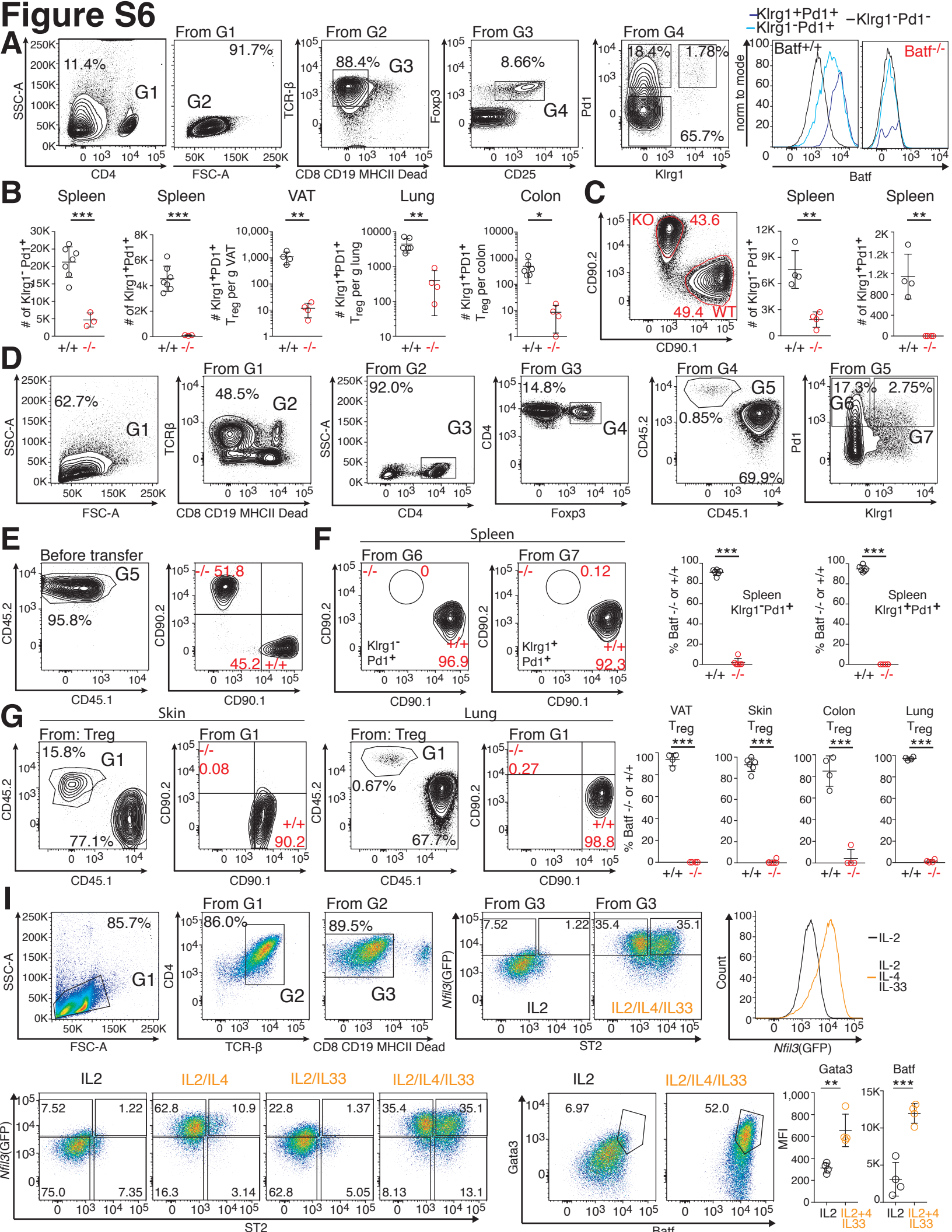
A
From G1
From G2
From G3
From G4
Klrg1+Pd1+
Klrg1-Pd1+
Klrg1-Pd1-
11.4%
G1
91.7%
G2
88.4%
G3
8.66%
G4
18.4%
1.78%
65.7%
SSC-A
CD4
FSC-A
TCR-β
CD8 CD19 MHCII Dead
Foxp3
CD25
Pd1
Klrg1
Batf+/+
Batf-/-
norm to mode
Batf
B
Spleen
Spleen
VAT
Lung
Colon
# of Klrg1-Pd1+
# of Klrg1+Pd1+
Klrg1+PD1+ Treg per g VAT
Klrg1+PD1+ Treg per g lung
Klrg1+PD1+ Treg per colon
+/+ -/-
C
KO
43.6
49.4
WT
CD90.2
CD90.1
Spleen
Spleen
# of Klrg1-Pd1+
# of Klrg1+Pd1+
D
From G1
From G2
From G3
From G4
From G5
62.7%
G1
48.5%
G2
92.0%
G3
14.8%
G4
0.85%
G5
17.3%
2.75%
G6
G7
69.9%
SSC-A
FSC-A
TCRβ
CD8 CD19 MHCII Dead
CD4
Foxp3
CD45.2
CD45.1
Pd1
Klrg1
E
Before transfer
G5
95.8%
-/- 51.8
45.2
+/+
CD45.2
CD45.1
CD90.2
CD90.1
F
Spleen
From G6
From G7
-/-
0
96.9
0.12
92.3
Klrg1-Pd1+
Klrg1+Pd1+
+/+
CD90.2
CD90.1
% Batf -/- or +/+
Spleen Klrg1-Pd1+
Spleen Klrg1+Pd1+
G
Skin
Lung
From: Treg
From G1
15.8%
G1
77.1%
-/-
0.08
90.2
0.67%
67.7%
0.27
98.8
CD45.2
CD45.1
CD90.2
CD90.1
% Batf -/- or +/+
VAT Treg
Skin Treg
Colon Treg
Lung Treg
I
From G1
From G2
From G3
From G3
85.7%
G1
86.0%
G2
89.5%
G3
7.52
1.22
35.4
35.1
IL2
IL2/IL4/IL33
SSC-A
FSC-A
CD4
TCR-β
CD8 CD19 MHCII Dead
Nfil3(GFP)
ST2
Count
IL-2
IL-2
IL-4
IL-33
IL2
IL2/IL4
IL2/IL33
IL2/IL4/IL33
7.52
1.22
75.0
7.35
62.8
10.9
16.3
3.14
22.8
1.37
62.8
5.05
35.4
35.1
8.13
13.1
IL2
IL2/IL4/IL33
6.97
52.0
Gata3
Batf
MFI
IL2
IL2+4
IL33

Figure S6. Batf and tissue Treg development, related to Figure 7. (**A**) Gating strategy used to identify Klrg1^{-}Pd1^{-}, Klrg1^{-}Pd1^{+} or Klrg1^{+}Pd1^{+} Treg cells in Batf$^{-/-}$ vs Batf$^{+/+}$ mice. G1: CD4^{+} T cells; G2: lymphocytes; G3: CD8^{-}CD19^{-}MHCII^{-}Dead^{-}TCRbeta^{+} T cells; G4: CD4^{+}CD25^{+} Treg cells. From G4, Klrg1^{-}Pd1^{-}, Klrg1^{-}Pd1^{+} or Klrg1^{+}Pd1^{+} Treg cells can be identified. Expression of Batf in all three populations of Batf$^{-/-}$ vs Batf$^{+/+}$ mice is shown as histogram to the right. (**B**) Total numbers of Klrg1^{-}Pd1^{+} or Klrg1^{+}Pd1^{+} Treg cells in spleens of Batf$^{-/-}$ vs Batf$^{+/+}$ mice (n=3-7, unpaired t-test). Right, total number of Klrg1^{+}Pd1^{+} Treg cells per g VAT, per g lung or per whole colon (unpaired t-test, n=4-6). (**C**) Total numbers of Klrg1^{-}Pd1^{+} or Klrg1^{+}Pd1^{+} Treg cells in spleens of mixed bone marrow chimeras with 50% Batf$^{+/+}$ and 50% Batf$^{-/-}$ bone marrow six weeks after bone marrow transfer (unpaired t-test, n=5). (**D**) Gating strategy to identify transferred CD45.1^{-}CD45.2^{+} Treg cells (mixed 50% CD90.1^{+}CD90.2^{-}Batf$^{+/+}$ and 50% CD90.1^{-}CD90.2^{+}Batf$^{-/-}$) in DT-treated CD45.1^{+}CD45.2^{-} Foxp3^{DTR} host animals two weeks after transfer. (**E**) Quality control of cells before transfer into congenic DT-treated recipient. (**F**) Presence of CD90.1^{+}CD90.2^{-}Batf$^{+/+}$ vs CD90.1^{-}CD90.2^{+}Batf$^{-/-}$ transferred Treg cells Klrg1^{-}Pd1^{+} or Klrg1^{+}Pd1^{+} Treg cells of spleens isolated from DT-treated host animals two weeks after transfer. Statistical verification across replicates to the right, gating (G6 and G7) derived from (E) (unpaired t test, n=4-6). (**G**) Presence of CD90.1^{+}CD90.2^{-}Batf$^{+/+}$ vs CD90.1^{-}CD90.2^{+}Batf$^{-/-}$ transferred Treg cells in lung or skin of DT-treated host animals two weeks after transfer with statistical verification across replicates (unpaired t test, n=4-6). (**I**) Gating strategy used to analyse Treg cells expanded with anti-CD3/28 microbeads and cytokines *in-vitro*. G1: lymphocytes; G2: CD4^{+}TCRbeta^{+} T cells; G3: CD8^{-}CD19^{-}MHCII^{-}Dead^{-}CD4^{+} T cells. From G3, *Nfil3*(GFP)$^{+}$ST2^{-} or *Nfil3*(GFP)$^{+}$ST2^{+} Treg cells can be identified. Histogram to the right depicts *Nfil3*(GFP) expression in both groups. Below, expression of *Nfil3*(GFP) vs ST2 in expanded Treg cells treated with IL-2, IL-2/IL-4, IL-2/IL-33, or IL-2/IL-4/IL-33. To the right, expanded Treg cells with fixation and permeabilization to detect intracellular proteins. MFI of Gata3 or Batf was extracted (unpaired t test, n=4). Data representative of two or more independent experiments or cell sorts.

Figure S7

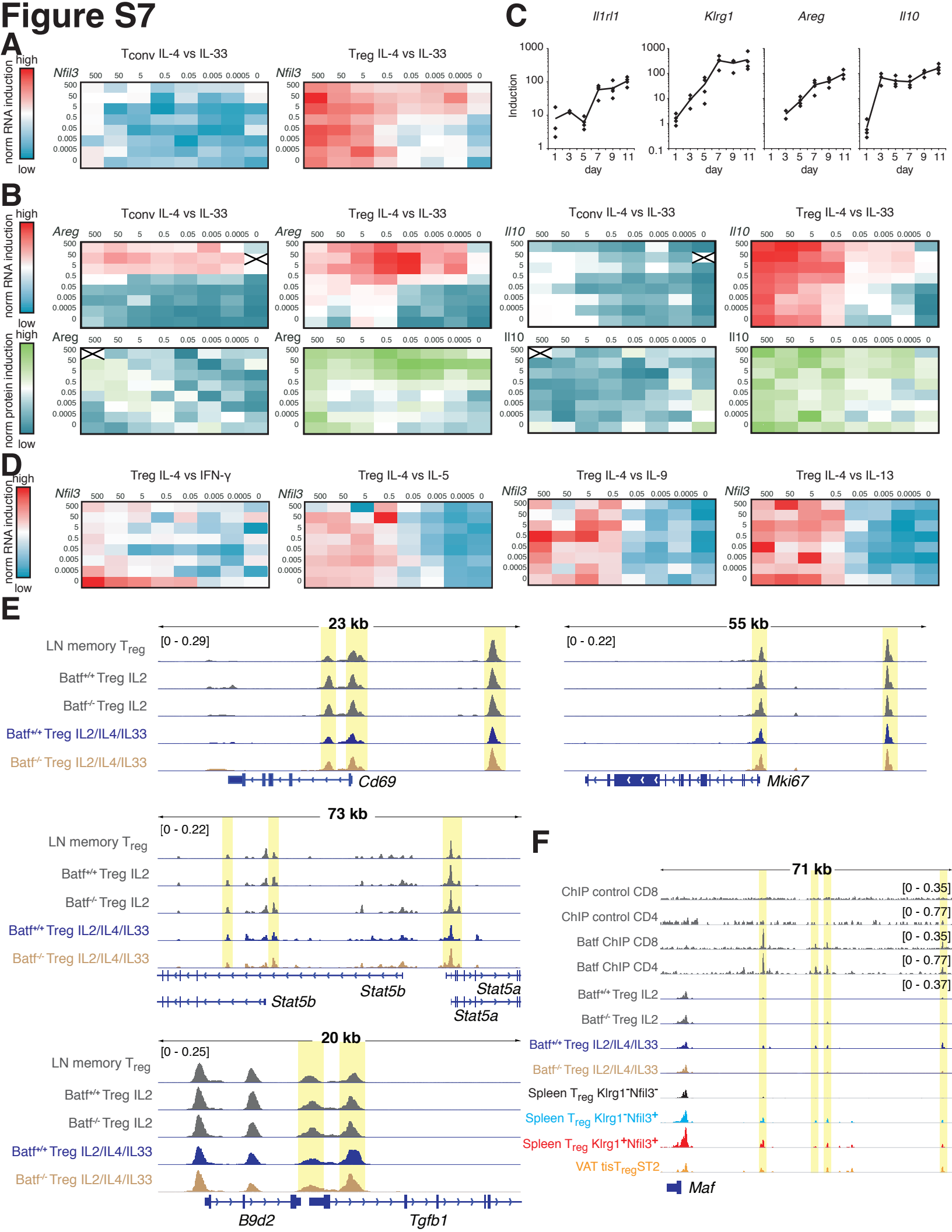
A
Tconv IL-4 vs IL-33
Treg IL-4 vs IL-33
Nfil3
norm RNA induction
high
low
B
Areg
Il10
norm protein induction
C
Il1rl1
Klrg1
Areg
Il10
Induction
day
D
Treg IL-4 vs IFN-γ
Treg IL-4 vs IL-5
Treg IL-4 vs IL-9
Treg IL-4 vs IL-13
E
23 kb
[0 - 0.29]
55 kb
[0 - 0.22]
73 kb
[0 - 0.22]
20 kb
[0 - 0.25]
LN memory Treg
Batf+/+ Treg IL2
Batf-/- Treg IL2
Batf+/+ Treg IL2/IL4/IL33
Batf-/- Treg IL2/IL4/IL33
Cd69
Mki67
Stat5b
Stat5a
B9d2
Tgfb1
F
71 kb
ChIP control CD8
ChIP control CD4
Batf ChIP CD8
Batf ChIP CD4
[0 - 0.35]
[0 - 0.77]
[0 - 0.37]
Spleen Treg Klrg1-Nfil3-
Spleen Treg Klrg1-Nfil3+
Spleen Treg Klrg1+Nfil3+
VAT tisTregST2
Maf

Figure S7. Batf and tissue Treg development, related to Figure 7. (**A**) Spleen Treg ($CD4^+CD25^+$*Foxp3*$(GFP)^+$) or Tconv ($CD4^+CD25^+$*Foxp3*$(GFP)^+$) cells were expanded with anti-CD3/28 microbeads and cytokines *in-vitro* for six days, followed by RNA isolation and cDNA synthesis. *Nfil3* gene expression was measured by RT-PCR and normalized to a house keeping gene (*Hprt*). Induction was calculated based on baseline *Nfil3* gene expression in untreated expanded Treg or Tconv cells and used to generate heatmap (colour code normalized to Treg and Tconv values) (n=1). (**B**) Cytokine titration of expanded Treg and Tconv as in (A), followed by measurement of *Areg* and Il10 RNA and protein (n=1). (**C**) Time course experiment with expanded Treg cells and a fixed dose of 100 ng/mL IL-4 and 100 ng/mL IL-33 and four replicates (n=4). Cytokines and media were exchanged on day 7. On day 1, 3, 5, 7, 9, and 11, RNA was extracted and gene expression of *Il1lr1*, *Klrg1*, *Areg* and *IL10* was measured by RT-PCR. Expression was normalized to control wells treated with IL-2 only (n=4). (**D**) Cytokine titration of expanded Treg cells as in (A-B), this time with IL-4 vs IFN-γ, IL-4 vs IL5, IL-4 vs IL-9, and IL-4 vs IL-13. Gene expression of *Nfil3* is shown (n=1). (**E**) ATAC-seq data for the *Cd69*, *Mki67*, *Stat5a*, *Stat5b*, and *Tgfb1* gene and associated promoter region with LN-derived $CD25^+$*Foxp3*$(GFP)^+CD44^+$ memory Treg (grey) as well as well as $Batf^{-/-}$ or control Treg cells treated with either IL-2 or IL-2/IL-4/IL-33 for six days in-vitro (grey, blue, light brown). Y-axis ATAC signal intensity, x-axis gene structure, with exons indicated as heightened bars and introns as line, arrows indicate gene direction. All datasets group-normalized to maximum peak height indicated in brackets. Overall display length indicated on top in kilobases (kb). Yellow box indicates area of interest (n=4). (**F**) ATAC-seq data for the *Maf* gene and associated promoter region as in (E), with top 4 lanes public dataset-derived Batf ChIP-seq data for CD4 or CD8 T cells including antibody control data (dark grey). Below, $Batf^{-/-}$ or control Treg cells treated with either IL-2 or IL-2/IL-4/IL-33 for six days in-vitro (grey, blue, light brown), spleen-derived $Klrg1^-$*Nfil3*$(GFP)^-$ Treg cells (black), spleen $Klrg1^-$*Nfil3*$(GFP)^+$ Treg cells (light blue), spleen $Klrg1^+$*Nfil3*$(GFP)^+$ Treg cells (red) and VAT-derived tisTregST2 (orange) (n=4). Data representative of independent experiments or cell sorts.